# Modeling Nonlinear and Time-Dependent Behaviors of Polymeric Sandwich Composites at Various Environmental Conditions

**Bentolhoda Davoodi, Antonio Gomez, Brian Pinto, Anastasia Muliana, and Valeria La Saponara**

## 1   Introduction

Sandwich structures consist of two thin facesheets (skins) with high stiffness and strength that are bonded to a relatively thick core. This sandwich system forms a lightweight structure with high strength and stiffness, and predominantly loaded under bending and/or twisting. The facesheets are usually made of metals or fiber-reinforced composite laminates, and the core is typically made of balsa wood, foams or honeycombs of polymeric or metallic material. The skins carry the tensile and compressive loads, and the core sustains the shear loads and holds the skins in positions away from the neutral axis of the structure, which maximizes the flexural stiffness of the structure [1]. Foams are among the most efficient core materials for weight-saving applications. The core and skin materials can be altered during manufacturing, which give sandwich constructions flexibility in design for various deflection requirements, bending stiffness and impact resistance requirements (see for example [2–4]).

Sandwich structures are widely used in many engineering applications, such as aircraft, naval structures and wind turbine blades. In wind turbine blades, sandwich composites with polymeric foam or honeycomb core and fiber-reinforced polymer (FRP) skins are a promising solution to obtain sufficiently lightweight blades with high bending stiffness and strength. In naval structures, sandwich composites with

B. Davoodi · A. Muliana (✉)
Department of Mechanical Engineering, Texas A&M University, College town, TX, USA
e-mail: amuliana@tamu.edu

A. Gomez · B. Pinto · V. La Saponara
Department of Mechanical and Aerospace Engineering, University of California, Davis, CA, USA
e-mail: vlasaponara@ucdavis.edu

foam core and fiber-reinforced composite skins are used to create a light, corrosion-resistant and stiff structure. In these applications, sandwich constructions are often subjected to various environmental conditions, which eventually alter their mechanical properties. Siriruk et al. [3, 4] studied the degradation in the mechanical behavior due to exposure to sea water in polymeric sandwich composites. They also showed that fracture toughness decreases after sea water exposure. Kolat et al. [5] studied the influence of core material selection and environmental conditions on the fracture toughness of sandwich structures with sea water conditioning, reporting that fracture toughness of systems with polyurethane and coremat core increases, while it decreases for wood and plywood core systems. Joshi et al. [6] analyzed the influence of moisture diffusion on viscoelastic sandwich composites deformation, and assumed the elastic and time-dependent properties of the foam core to depend on the moisture concentration. They conducted coupled analyses of moisture diffusion and deformation to predict the viscoelastic sandwich systems performance.

Due to the presence of polymers in sandwich composites, these structures show quite pronounced viscoelastic response, which can influence their overall life performance. Du et al. [7] determined the creep properties of sandwich composites, and showed that higher relative humidity produced a significant acceleration in creep strain. Shenoi et al. [8] studied creep for a typical sandwich structure using a Burger model and a power law model, and compared the model with experimental results. Garrido et al. [9] conducted experimental and analytical studies on the creep behavior of sandwich composite to propose a creep model to simulate the sandwich panel's creep deformations in long-term.

Scudamore and Cantwell [10] showed that long term sea water exposure caused degradation of the bond between the epoxy matrix and the aluminum core, and led to skin-core interface cracks. Li and Weitsman [11] also characterized the fracture toughness of dry and wet foams (after exposure to sea water), and showed that absorption of sea water increases the toughness of the foam materials due to the softening of the wet polymeric foam, as the glass transition temperature was reduced. Ishai et al. [12] and Ishiaku et al. [13] showed the significant strength reduction of foams and polymeric sandwich composite due to moisture absorption. Belingardi et al. [14] characterized polymeric sandwich composites properties using a series of static/quasi-static tests and showed the dependency of the structural response of the sandwich to the foam core strength properties. Kim et al. [15] and Jeon et al. [16] investigated a multi-scale experimental and modeling approaches on the time dependent response of different constituents of sandwich composite. They characterized how their interaction impacts the overall creep performance of smart polymer sandwich constructions.

In the current study, we conduct experiments to investigate the mechanical behaviors of polymeric sandwich composites and their constituents, with the goal of understanding the effect of the constituents' response on the overall performance of sandwich composites. The sandwich composites and their constituents are also subjected to different environmental conditions (dry and wet due to immersion in fluid, at the temperature of 50 °C). See discussion in Fan et al. [17–19]. We also model the mechanical response of sandwich composites and their constituents. A

previously developed nonlinear viscoelastic material model is used to simulate bending test for foam beams. The constitutive model is implemented in a user subroutine (UMAT) in ABAQUS FE analysis. FE analysis is then used to describe mechanical responses of the sandwich composites and their constituents.

## 2    Experiments

Tests were conducted on materials that are known to be time-dependent: polymeric foams and sandwich composites made with those foams. In particular, there were two sandwich composite systems, which were manufactured using out-of-autoclave Vacuum Assisted Resin Transfer Molding. The layups were selected as [90]$_4$, to ensure a higher viscoelastic response of the material. The first system is glass fiber-reinforced polymer (GFRP) having E-glass fibers (quasi-unidirectional Vectorply E-LR 0908) and epoxy (Pro-set LAM 125/LAM237, with an infusion ratio of 100:28 resin:hardener by weight ratio for the skins), and polyurethane (PU) foam, (General Plastics FR-3704, nominal thickness 19.1 mm) for the core. We refer to this system as "GFRP/PU". The resin cure cycle consisted of 14 h at room temperature, followed by 8 h at 82 °C in a convection oven. This system was studied as an example of a sandwich for wind turbine applications. The second system is a sandwich with skins made of carbon fibers (quasi unidirectional Torayca T700S) and vinylester (Hetron FR 992, with additives cobalt naphthenate and methyl ethyl ketone peroxide, with an infusion ratio of 100:0.15:1.25 by volume), and a polyvinylchloride (PVC) foam core (DIAB Divinycell H100, nominal thickness 25.5 mm). We refer to this system herein as "CFRP/PVC". The vinylester had a cure cycle of 45 min at room temperature and 4 h at 82 °C. This system was considered for naval application.

The two sandwich systems were subjected to two different conditions: the GFRP/PU sandwich and its constituents (GFRP skins and PU) were immersed in deionized water at 50 °C (herein named as "Condition 1"), while the CFRP/PVC sandwich and its constituents (CFRP skins and PVC foam) were immersed in artificial sea water at 50 °C (herein named as "Condition 2"). The expression "artificial sea water" stands for a solution of deionized water and 3.5% wt. content of NaCl. Table 1 provides the immersion testing conditions for the samples, with different durations dictated by experimental constraints. "Condition 1" and "Condition 2" are meant to simplify the discussion in this paper, with the understanding that each condition includes a time range for skins, foam and sandwich samples.

**Table 1**  Immersion testing conditions

| Temperature | Immersion fluid | Sample | Duration (days) |
| --- | --- | --- | --- |
| 50 °C | Deionized water | GFRP skins, PU foam | 150 |
| 50 °C | Deionized water | GFRP/PU sandwich | 188 |
| 50 °C | Artificial Sea water | CFRP skins, PVC foam | 107 |
| 50 °C | Artificial Sea water | CFRP/PVC sandwich | 53 |

**Fig. 1** (Left) three-point bending test on PU foam; (right) four-point bending test on PVC foam

Baseline and conditioned sandwich composites and their constituents were subjected to several types of mechanical tests on a hydraulic axial machine (MTS 810). Typically, bending tests (quasi-static, creep and stress relaxation) were conducted on foam and sandwich samples, while quasi-static axial tests were run for monolithic FRP samples, following the requirements of the appropriate ASTM standard. The selection between creep and stress relaxation was based on the load capacity of the sample under exam. The bending test setups are shown in Fig. 1. The bending tests consist of three- and four-point bending tests, depending on the top part of the fixture (wedge with a roller, or fixture with two rollers). In some cases, the wedge became unavailable, leading to a number of four-point bending tests on conditioned samples, while baseline samples had been tested under three-point bending. However, the model presented in this paper is capable of capturing the different bending conditions, and the softening of the samples as a result of conditioning is successfully computed.

## 3 Constitutive Material Models for the Constituents

### 3.1 Nonlinear Viscoelastic Model for Foam

The nonlinear viscoelastic model for the polymeric foams is based on the quasi-linear viscoelastic (QLV) model of Muliana et al. [20]. The QLV constitutive model was originally proposed by Fung [21]. The polymers are assumed to be isotropic and homogeneous. From the experimental observations, the magnitude of strain is relatively small, thus engineering stress and strain measures are considered in the model.

The three-dimensional (3D) QLV model for isotropic materials is shown in Eq. (1):

$$\sigma_{ij}(t) = \int_{0^-}^{t} 2G(t-s)\frac{dF_{ij}}{ds}ds + \delta_{ij}\int_{0^-}^{t} \lambda(t-s)\frac{dF_{kk}}{ds}ds \tag{1}$$

where $\delta_{ij}$ is the Kronecker delta and $\lambda$ is a material parameter, one of the two Lame's constants, defined as:

$$\lambda = K_B - (2/3)G \tag{2}$$

where $G$ and $K_B$ are the shear modulus and bulk modulus, respectively. These material parameters depend on time. The corresponding Poisson's ratio, $\nu_0$, is assumed to be constant, and this leads to:

$$G(t) = \frac{E(t)}{2(1 + \nu_0)} \tag{3}$$

$$K_B(t) = \frac{E(t)}{3(1 - 2\nu_0)} \tag{4}$$

where $E(t)$ is the extensional relaxation modulus of the polymer, expressed as:

$$E(t) = E_\infty + \sum_{n=1}^{N} E_n e^{\frac{-t}{\tau_{Rn}}} \tag{5}$$

$\tau_{Rn}$ is the characteristic of relaxation time, $E_n$ is the coefficient in the time-dependent part, $N$ is the number of terms in the Prony series, and $E_\infty$ is the relaxed modulus. The nonlinear strain measure in a generalized 3D QLV model is defined as:

$$F(\bar{\varepsilon}(t)) = A\left[e^{B\bar{\varepsilon}(t)} - 1\right] \tag{6}$$

$$\bar{\varepsilon}(t) = \sqrt{\varepsilon_{ij}\varepsilon_{ij}} \tag{7}$$

$$\frac{dF_{ij}}{ds} = ABe^{B\varepsilon^-(t)}\frac{d\varepsilon_{ij}}{ds} \tag{8}$$

$$\frac{dF_{kk}}{ds} = ABe^{B\varepsilon^-(t)}\frac{d\varepsilon_{kk}}{ds} \tag{9}$$

With the above nonlinear strain measures and $E_o = AB$, the constitutive relation becomes

$$\sigma_{ij}(t) = 2C_1 \int_{0^-}^{t} K(t-s)E_0 e^{B\bar{\varepsilon}}\frac{d\varepsilon_{ij}}{ds}\,ds + \delta_{ij}C_2 \int_{0^-}^{t} K(t-s)E_0 e^{B\bar{\varepsilon}}\frac{d\varepsilon_{kk}}{ds}\,ds \tag{10}$$

where

$$C_1 = \frac{1}{2(1 + \nu_0)} \tag{11}$$

$$C_2 = \frac{1}{3(1 + 2\nu_0)} - \frac{1}{3(1 + \nu_0)} \tag{12}$$

The normalized time dependent function is

$$K(t) = K_\infty + \sum_{n=1}^{N} K_n e^{\frac{-1}{\tau_{Rn}}} \tag{13}$$

$$K(0) = K_\infty + \sum_{n=1}^{N} K_n = 1.0 \tag{14}$$

The above model is implemented in a user material subroutine (UMAT) of ABAQUS FE analyses. The numerical algorithm is discussed in Muliana et al. [20].

## 3.2 Elastic-Plastic Model for Skins

The elastic-plastic material model [22, 23] is used to simulate the behavior of FRP skins in the sandwich composite. A rate-independent plasticity model is considered in order to capture the elastic-plastic response of the FRP skins. From the experimental observation for mechanical deformation of the FRP skins, the strains are relatively small, which allow for additive decompositions of the elastic and plastic deformations. Thus, the total strain rate is given as:

$$\dot{\boldsymbol{\varepsilon}} = \dot{\boldsymbol{\varepsilon}}^{el} + \dot{\boldsymbol{\varepsilon}}^{pl} \tag{15}$$

where $\boldsymbol{\dot{\varepsilon}}$ is the total (mechanical) strain rate, $\dot{\boldsymbol{\varepsilon}}^{el}$ is the elastic strain rate, and $\dot{\boldsymbol{\varepsilon}}^{pl}$ is the plastic strain rate. Equation (15) is an approximation when the elastic strains are infinitesimal. The rate of deformation tensor is work-conjugate to the Cauchy stress tensor and is used to define the strain rate:

$$\dot{\boldsymbol{\varepsilon}} = \frac{1}{2} \left( \frac{\partial v}{\partial x} + \left( \frac{\partial v}{\partial x} \right)^T \right) \tag{16}$$

The linear elastic isotropic constitutive equation can be written as

$$\boldsymbol{\sigma} = \boldsymbol{C} : \boldsymbol{\varepsilon}^{el} \tag{17}$$

where C denotes the fourth-order elastic stiffness tensor.

The yield function is often expressed in terms of an equivalent stress, i.e. a scalar measure of the magnitude of the Cauchy stress tensor. Von Mises equivalent stress is:

$$\bar{\sigma} = \bar{\sigma}[\boldsymbol{\sigma}] = \sqrt{\frac{3}{2}\boldsymbol{S} : \boldsymbol{S}} \tag{18}$$

where the deviatoric tensor is

$$\boldsymbol{S} = dev[\boldsymbol{\sigma}] = \boldsymbol{\sigma} - \frac{tr[\boldsymbol{\sigma}]}{3}\boldsymbol{I} \tag{19}$$

Using Von Mises equivalent stress definition, the yield function is written as:

$$f\left[\boldsymbol{\sigma}, \bar{\varepsilon}^{pl}\right] = \bar{\sigma}[\boldsymbol{\sigma}] - k\left[\bar{\varepsilon}^{pl}\right] \tag{20}$$

and the yield surface is

$$f\left[\boldsymbol{\sigma}, \bar{\varepsilon}^{pl}\right] = 0 \tag{21}$$

The $k\left[\bar{\varepsilon}_{pl}\right]$ term shows the isotropic hardening. The hardening parameters are state variables that are introduced to allow the model to describe some of the complexity of the inelastic response of real materials. In perfect plasticity, which is the simplest plasticity model, the yield surface acts as a limit surface and there are no hardening parameters. In this study, from observed experimental tests of FRP skins, an elastic-perfectly plastic deformation model is adopted.

# 4   Results and Discussion

As mentioned earlier, two systems of sandwich composites (GFRP/PU and CFRP/PVC) and their constituents have been tested. The sandwich composites and foams were tested under bending, while the fiber reinforced polymeric skins were tested under uniaxial tension. The constitutive models discussed above are used to describe the mechanical response of the skins and foams. These models are implemented in finite element (FE); the response of baseline and conditioned sandwich composites under bending is simulated and compared to the experimental results. Quasi-static ramp tests were performed on skins (under tension), foam and sandwich composites (under bending). In addition, creep/relaxation tests under bending were performed for the foam and sandwich composites. The overall goals are: (1) to understand the different response of the constituents in sandwich composites and their effects on the overall mechanical response of sandwich composites; (2) to investigate the effect of environmental conditions on the mechanical response of composites and their constituents.

## 4.1  Uniaxial Tension Response of Skins

Uniaxial static tests are performed on baseline (dry) GFRP and CFRP skins, and conditioned ("wet", removed from immersion tanks and not dried) specimens (GFRP skins under Condition 1, CFRP skins under Condition 2). Samples had a 25.7 mm nominal width, consistent with ASTM standard for uniaxial testing, and a nominal thickness of 1.5 mm. The experimental results and simulations are shown in Figs. 2, 3, 4 and 5. The calibrated material parameters are given in Table 2. From Table 2, it is seen that, due to degradation caused by the immersion in fluid at 50 °C,
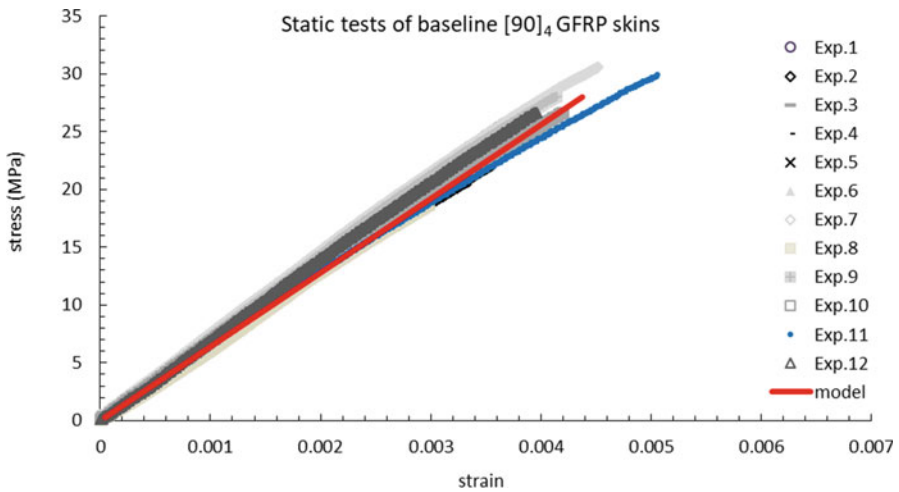


**Fig. 2** Static uniaxial tests and model of baseline GFRP skins with [90]$_4$ layup
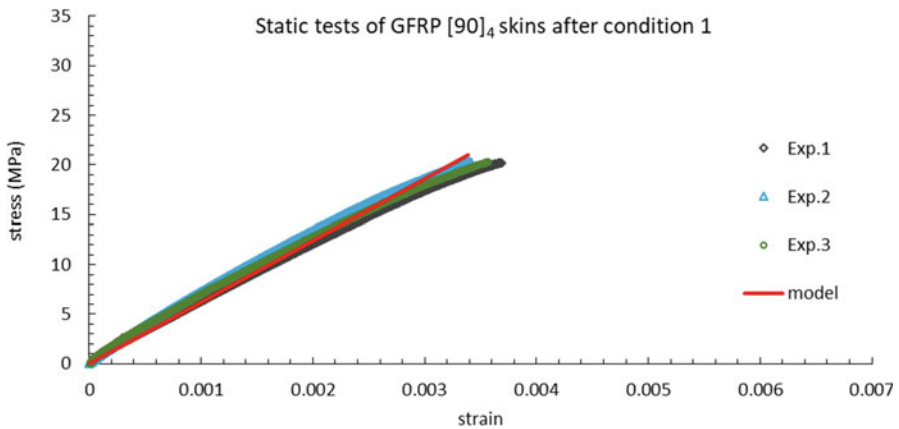


**Fig. 3** Static uniaxial tests and model of conditioned GFRP skins with [90]$_4$ layup
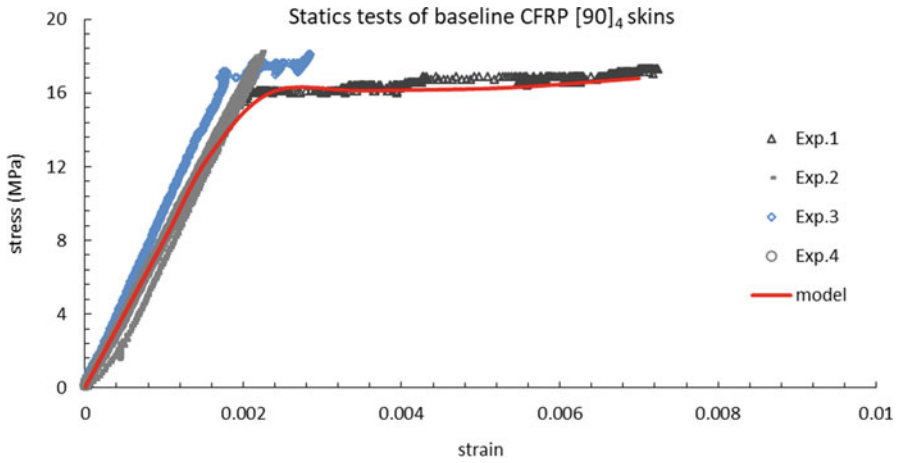
**Fig. 4** Static uniaxial tests and model of baseline CFRP skins with [90]₄ layup
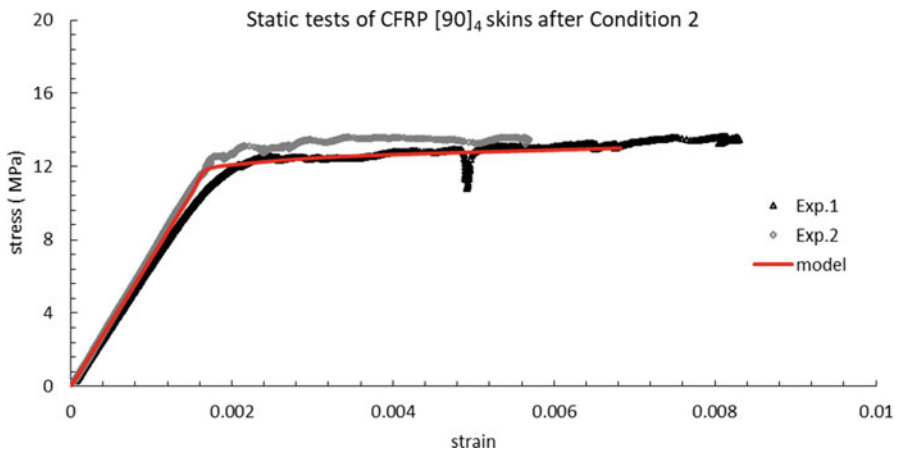


**Fig. 5** Static uniaxial tests and model of conditioned CFRP skins with with [90]₄ layup

**Table 2** Mechanical properties of GFRP and CFRP skins

| Material | | $E$ (MPa) | $\sigma_y$ (MPa) |
|---|---|---|---|
| Glass/epoxy | Baseline | 6800 | – |
| | After Condition 1 | 6200 | – |
| Carbon/vinylester | Baseline | 8000 | 16 |
| | After Condition 2 | 7000 | 12 |

the monolithic composites become softer, which is indicated by a reduction in the elastic modulus. The CFRP composite shows inelastic deformations (elastic-plastic behavior) before failure, while the GFRP composite shows a nearly linear elastic response. Fluid immersion also decreases the yield stress in GFRP.

## 4.2 Bending Tests on Foams

The FE analysis is used to simulate bending in polymeric foams. The nominal dimensions of the foam test specimens are 150 mm length × 57.3 mm width × 19 mm thickness for PU and 150 mm length × 57.2 mm width × 25.5 mm thickness for PVC. Loading was applied consistently with the geometry of the fixture (either at the middle of the beam, for three-point bending tests, or at two loading locations, at 30 mm from beam supports, for the four-point bending tests, Fig. (6). The simply supported mechanical boundary conditions are assumed for both three- and four-point bending models, based on the presence of rollers in the actual fixture. In order to model a simply supported beam, one side of the beam is constrained to prevent displacement in vertical/lateral (y) direction and on the other side of the beam the displacements in axial (x) and lateral (y) directions are restricted. The FE mesh of the beam is generated using the nonlinear three dimensional continuum elements (C3D20) and a convergence study has been performed in order to determine the number of elements required in the analyses.

The load-displacement plots for the foam samples subjected bending tests, and their model for the baseline state and the conditioned state (after immersion) are shown in Figs. 7, 8, 9 and 10. The overall responses of foam under bending are nonlinear. Using the experiments (Figs. 7, 8, 9 and 10), material parameters are calibrated. The material properties are shown in Table 3. The nonlinear constitutive model based on QLV discussed above is used to describe the nonlinear quasi-static ramp response, without incorporating the time-dependent parameters. From Table 3, we can see that by immersion in fluid at elevated temperature, the stiffness of foam samples is reduced.



**Fig. 6** Boundary conditions of three- and four-point bending tests
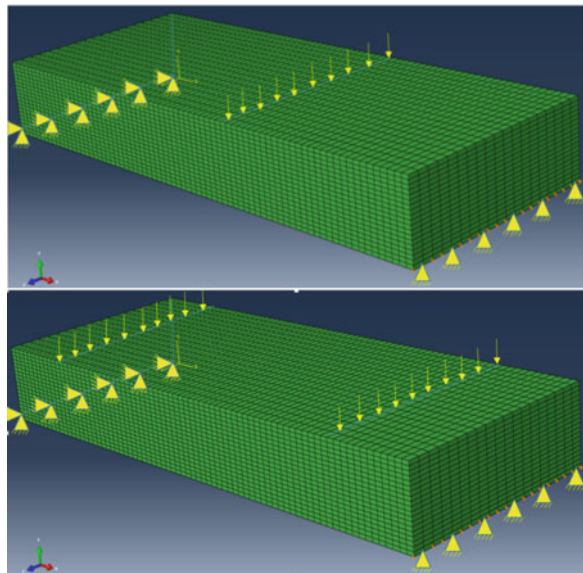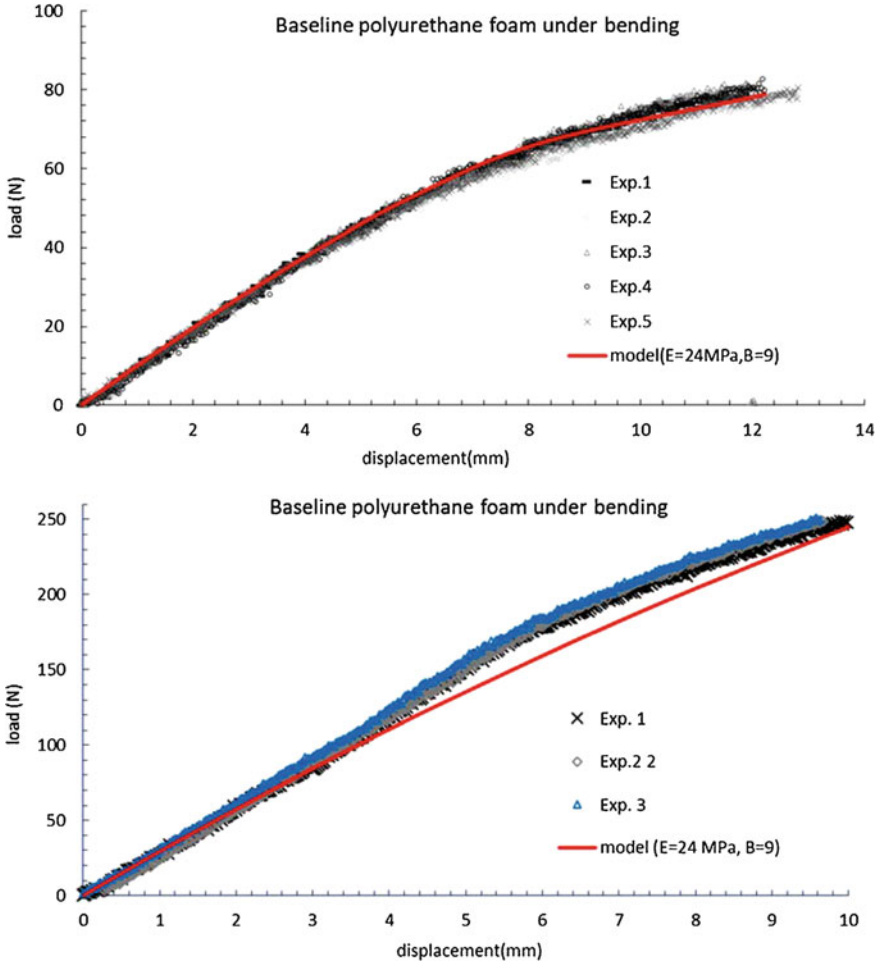
**Fig. 7** Static bending tests and model of baseline polyurethane foam under three-point bending (top) and four-point bending (bottom)

## 4.3 Bending Response of Sandwich Composites

In the previous sections, FE analyses were performed for skins and foam cores. In this part, the response of the sandwich composite under static bending will be modeled. The specimen is a beam consisting of foam core and fiber-reinforced polymer skin, with loading perpendicular to fiber direction. The first system is a GFRP/PU sandwich composite with nominal dimensions $150 \times 26 \times 22$ mm$^3$ for baseline conditions, and $150 \times 57 \times 22$ mm$^3$ for immersion conditions, with a skin thickness of 2 mm. The second system is a CFRP/PVC sandwich composite with nominal dimensions $150 \times 26 \times 27.8$ mm$^3$ for baseline condition, and
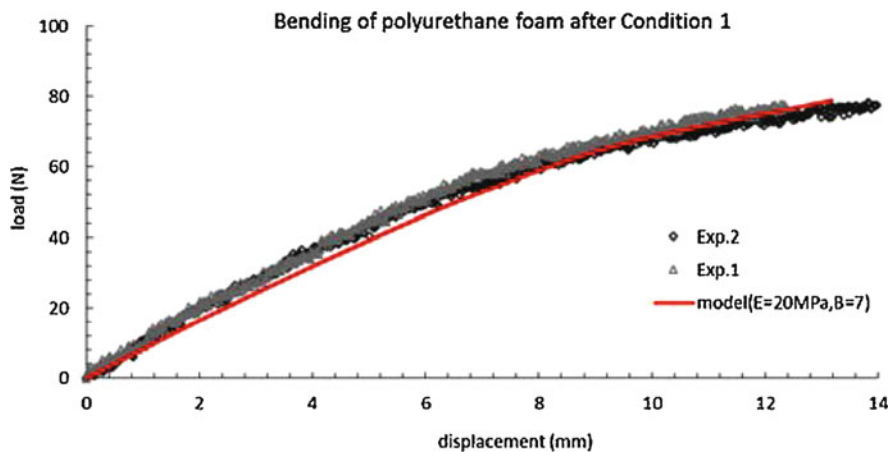
**Fig. 8** Static bending tests (3 point bending) and model of conditioned polyurethane foam
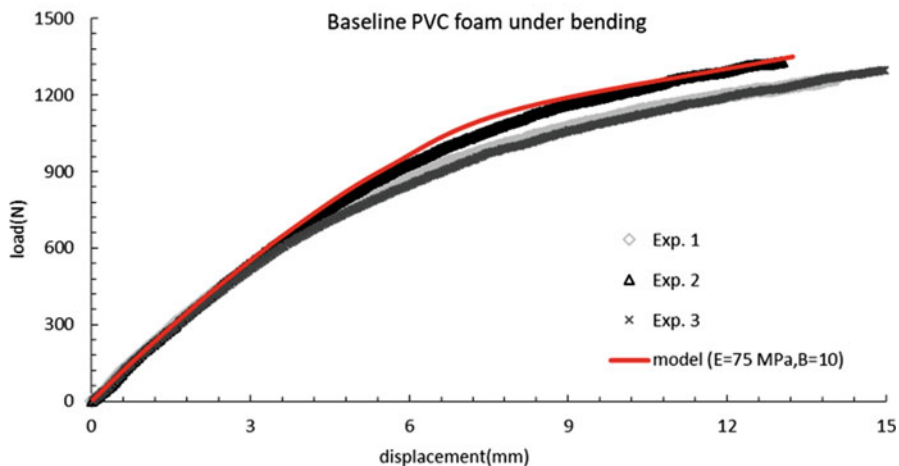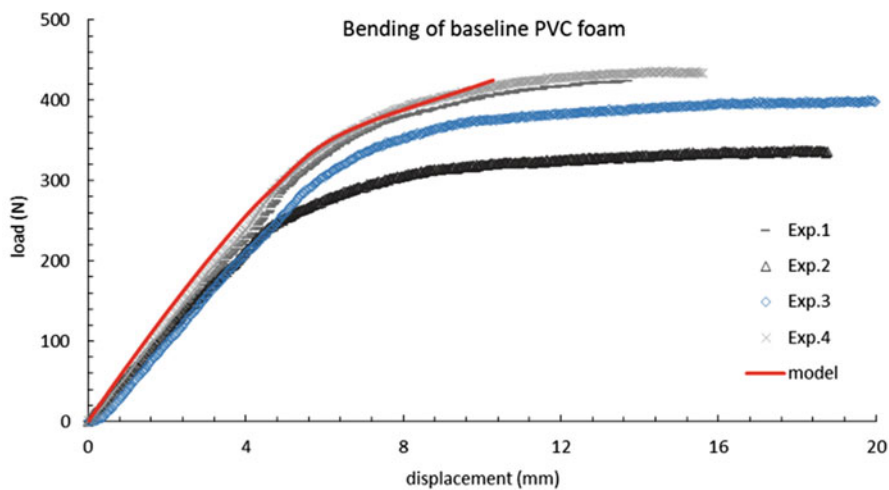


**Fig. 9** Static bending tests and model of baseline PVC foam under (top) three-point bending and (bottom) four-point bending
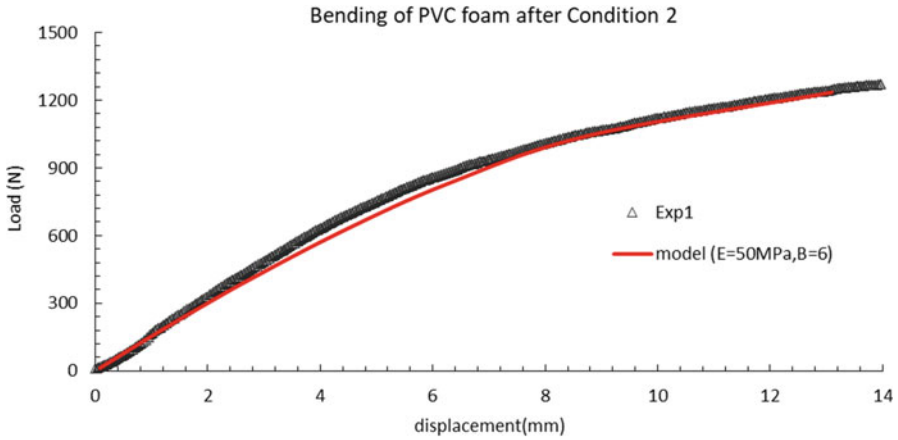
**Fig. 10** Static bending tests (four-point bending) and model of conditioned PVC foam

**Table 3** Computed material properties for foams

| Material | | E (MPa) | B |
|---|---|---|---|
| PU foam | Baseline | 24 | 9 |
| | After Condition 1 | 20 | 7 |
| PVC foam | Baseline | 75 | 7.2 |
| | After Condition 2 | 50 | 6 |

$150 \times 57.327.8$ mm$^3$ for immersion conditions, with a skin thickness of 1 mm. To simulate the sandwich composite in FE, the foam and skin are separated using partitioning. The nonlinear three-dimensional continuum elements (C3D20) are used, and a convergence study is carried out for the proper number of elements. Note that the width of the condition specimens is about twice the width of the baseline specimens. This difference in width will affect the load magnitude applied to the sandwich composites.

The nonlinear responses of the sandwich composites are shown in Figs. 11, 12, 13 and 14 for the two different systems. In the quasi-static tests for baseline GFRP/PU sandwich composites, there is good agreement between model and experimental results before failure at a deflection of about 4 mm. In the conditioned GFRP/PU sandwich composites, there is also a good agreement between model and experiments before a crack occurs in the sandwich, with a resulting drop in load around a 4 mm displacement. The model of the quasi-static test on baseline CFRP/PVC sandwich composites is in acceptable agreement with the experiments. The result of experimental tests on conditioned CFRP/PVC sandwiches shows that a delamination occurs after loading. By taking into account the delamination around 350 N loading, the model captures the experimental behavior. In the GFRP/PU sandwich composites, failure is observed mostly due to foam cracking, while in the CFRP/PVC sandwich composites failure is governed by skin-core delamination. The different responses in these two sandwich composites are associated with the responses of the constituents. The PVC foam core shows a much stronger and stiffer
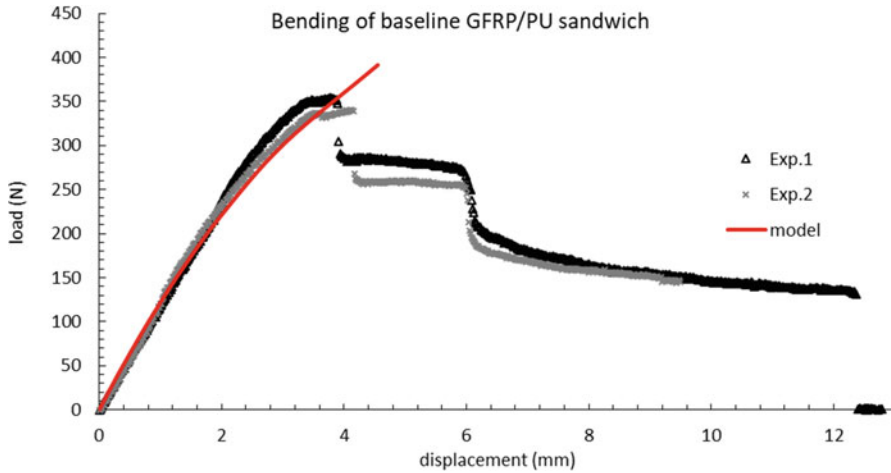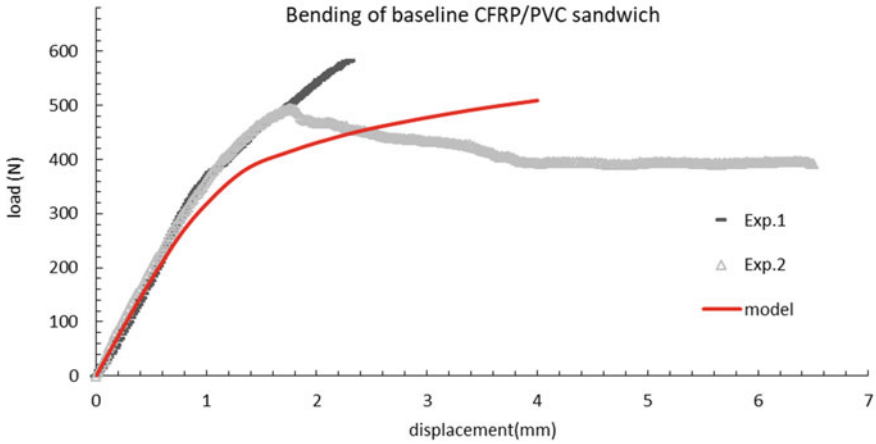
**Fig. 11** Static bending tests (three-point bending) and model of baseline GFRP/PU sandwich composites
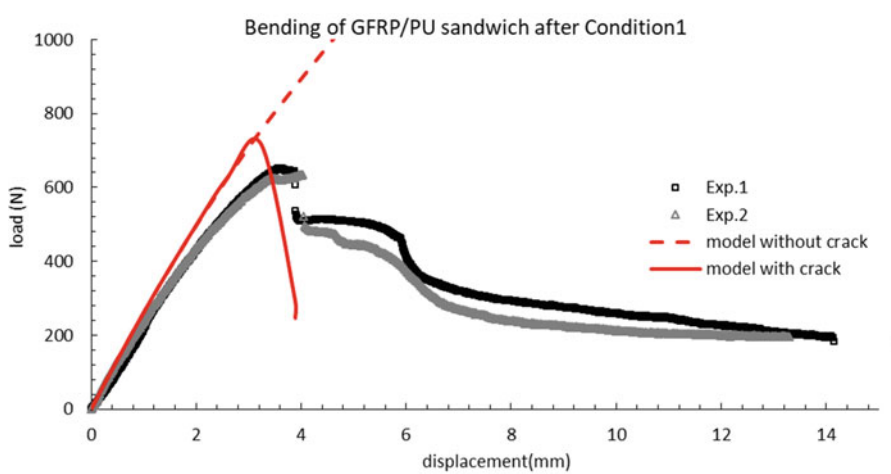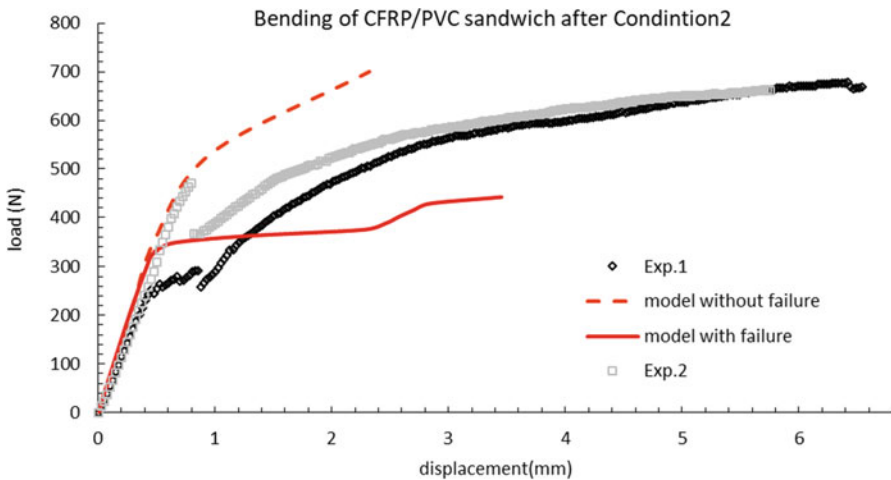


**Fig. 12** Static bending tests (three-point bending) and models of conditioned GFRP/PU sandwich composites

response than the PU core, which explains that cracking is unlikely to occur in PVC foam core. The CFRP skins show a ductile behavior; thus, higher deformation in the skins combined with foam core of high stiffness and strength leads to skin-core delamination. The GFRP skins indicate a brittle-like behavior, which explains that failure in GFRP/PU sandwich is due to breaking of the skin on the tension face,

**Fig. 13** Static bending tests (three-point bending) and model of baseline CFRP/PVC sandwich composites



**Fig. 14** Static bending tests (three-point bending) and model of baseline CFRP/PVC sandwich composites

followed by cracking of the foam. Figures 15 and 16 illustrate the axial stress and strain contours in the GFRP/PU sandwich composite and CFRP/PVC sandwich composite, respectively, from FE simulation of conditioned sandwich specimens. Due to cracks, the tensile stress in the GFRP skin drops, leading to increase in the axial strain in the foam. Delamination in the CFRP/PVC sandwich composites leads to much higher strain in the foam core.
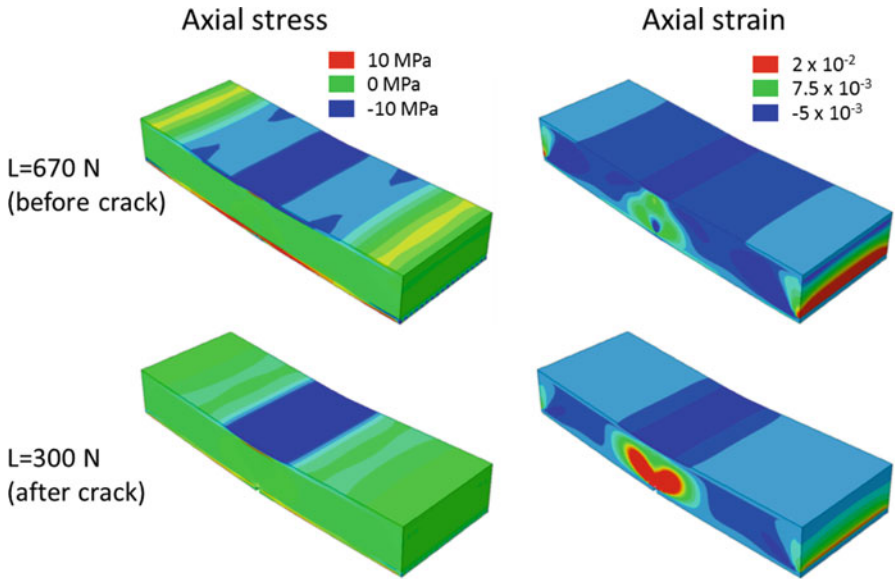
**Fig. 15** Axial stress and strain contours in GFRP/PU sandwich composite before and after crack (from simulation)
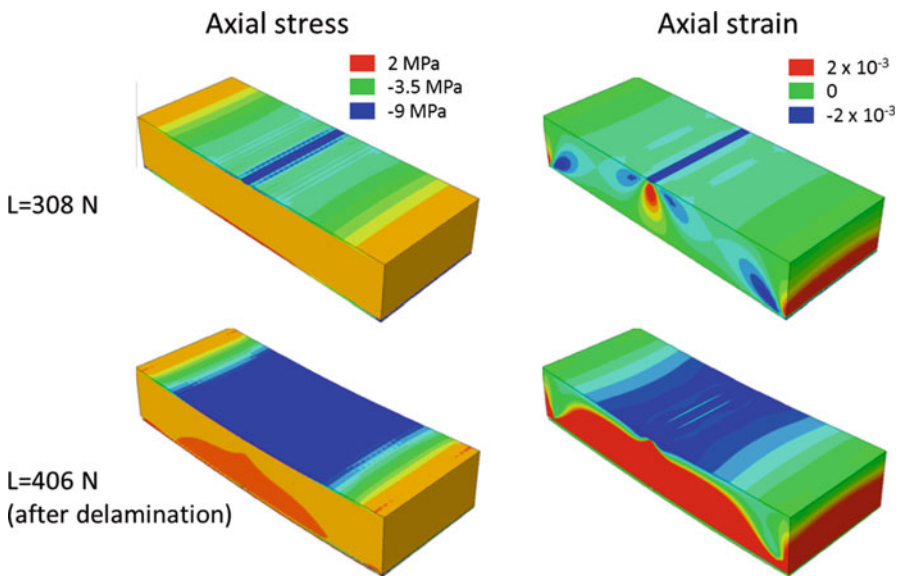


**Fig. 16** Axial stress and strain contours in CFRP/PVC sandwich composite before and after delamination (from simulation)

## 4.4 Time-Dependent Response of Foams and Sandwich Composites

To determine the time-dependent properties of the foam core, creep and stress relaxation tests under bending were conducted (Figs. 17, 18, 19 and 20). The calibrated time-dependent parameters for the PU and PVC cores in terms of the normalized time-dependent parameters in Eq. (13) are given in Table 4. It is seen that
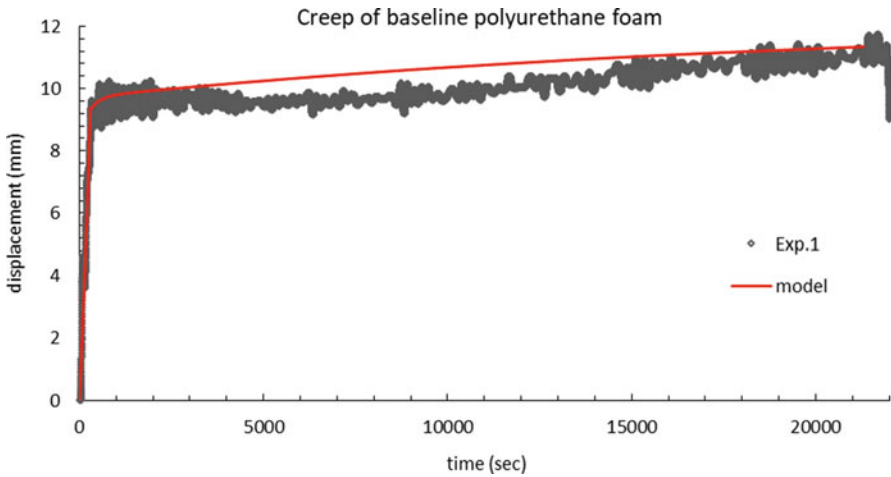


**Fig. 17** Creep response under bending (three-point bending) of baseline polyurethane foam
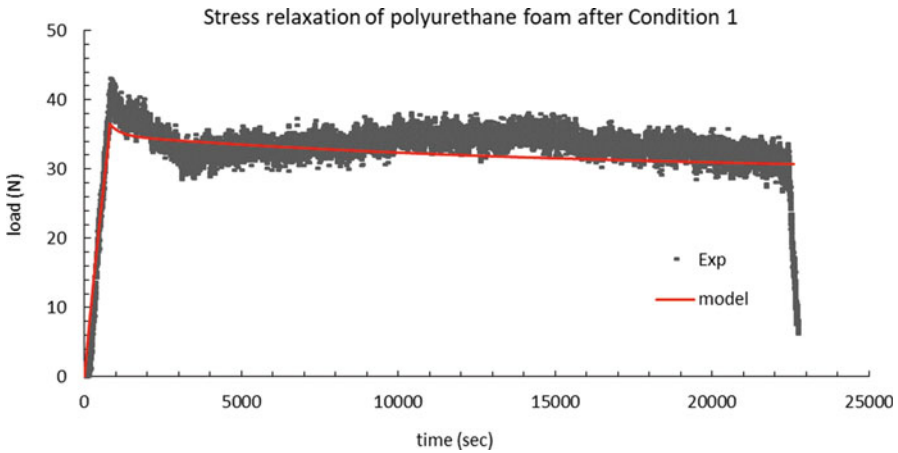


**Fig. 18** Stress relaxation response under bending (three-point bending) and model of conditioned polyurethane foam
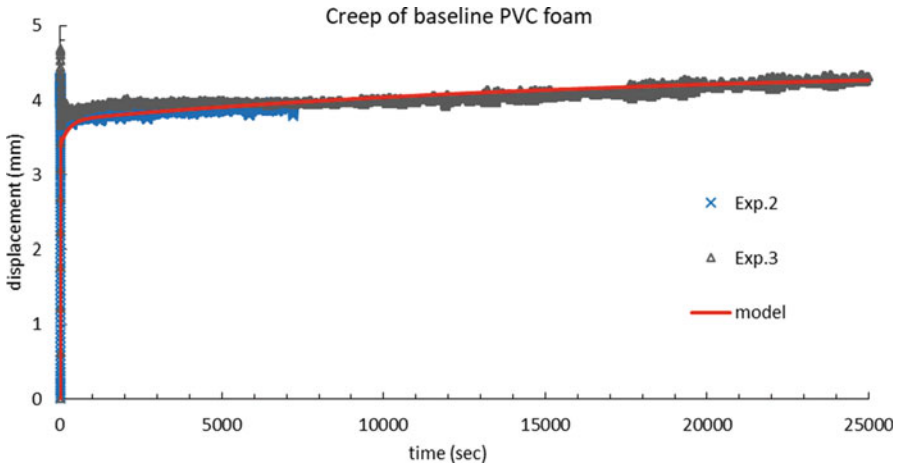
**Fig. 19** Creep response under bending (three-point bending) and model of baseline PVC foam
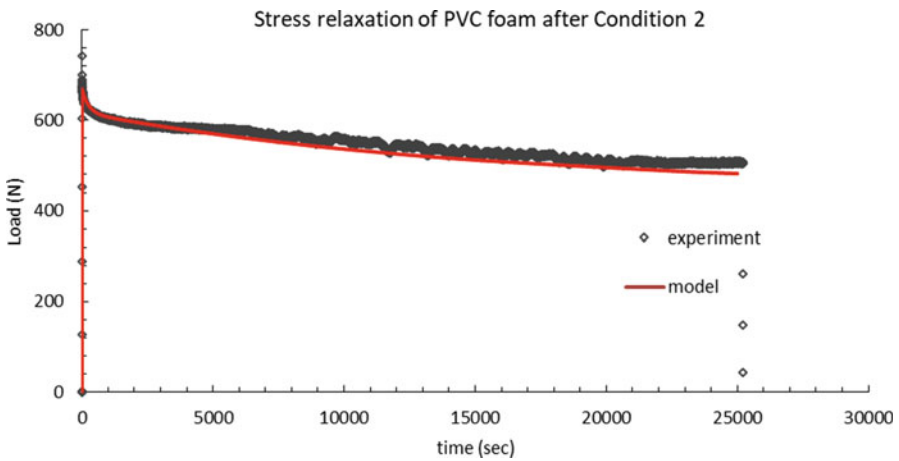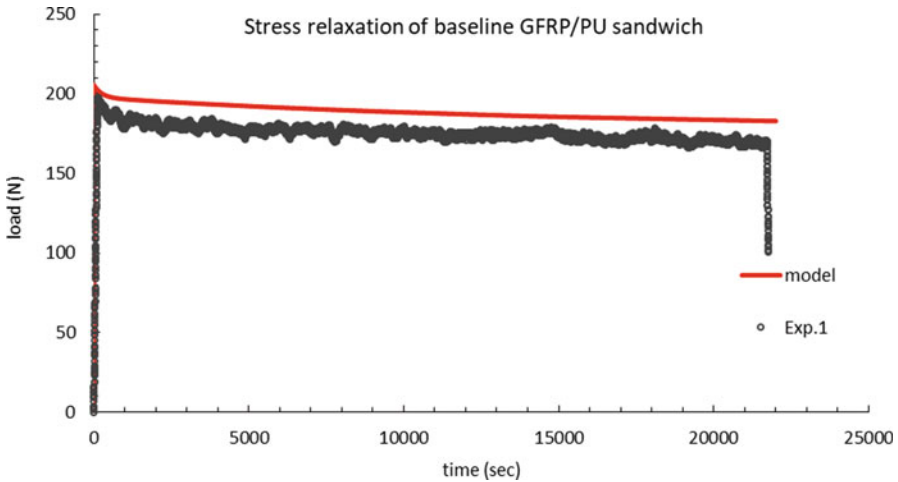


**Fig. 20** Stress relaxation under bending (four-point bending) and model of conditioned PVC foam

**Table 4** Normalized time-dependent foam properties

| Material/Condition | $K_\infty$ | $K_1$ | $K_2$ | $\tau_1$(sec) | $\tau_2$(sec) |
|---|---|---|---|---|---|
| Baseline PU foam | 0.83 | 0.05 | 0.12 | 250 | 15,000 |
| Conditioned PU foam | 0.74 | 0.1 | 0.16 | 350 | 15,000 |
| Baseline PVC foam | 0.75 | 0.1 | 0.15 | 250 | 15,000 |
| Conditioned PVC foam | 0.5 | 0.12 | 0.38 | 250 | 15,000 |

the long-term relaxation modulus decreases in both PU and PVC foams upon conditioning in their respective fluids at 50 °C.

FE analyses are used to simulate the creep/relaxation response in sandwich composites, and are compared to experimental results. In this part, we used the material properties in Table 4 for capturing the time-dependent response of sandwich composites. The stress relaxation test and simulation results are shown in Figs. 21 and 22 for the GFRP/PU sandwich composites, and in Figs. 23 and 24 for CFRP/
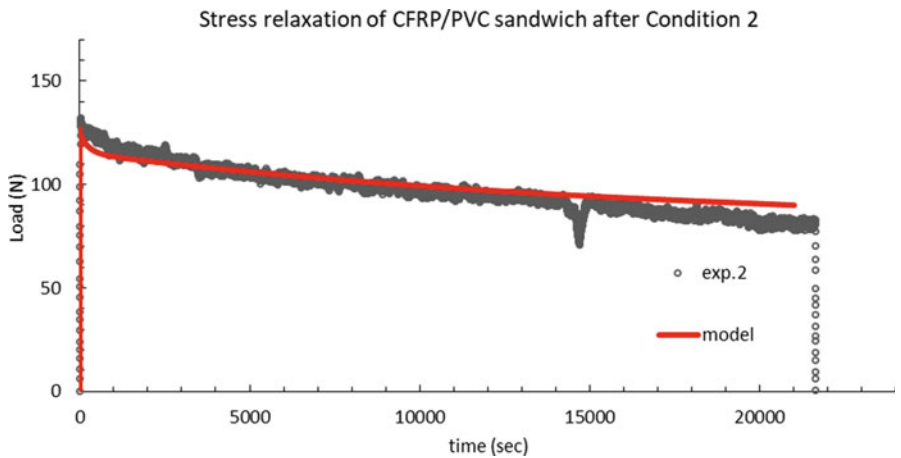


**Fig. 21** Stress relaxation under bending tests (three-point bending) and model of baseline GFRP/PU sandwich composites
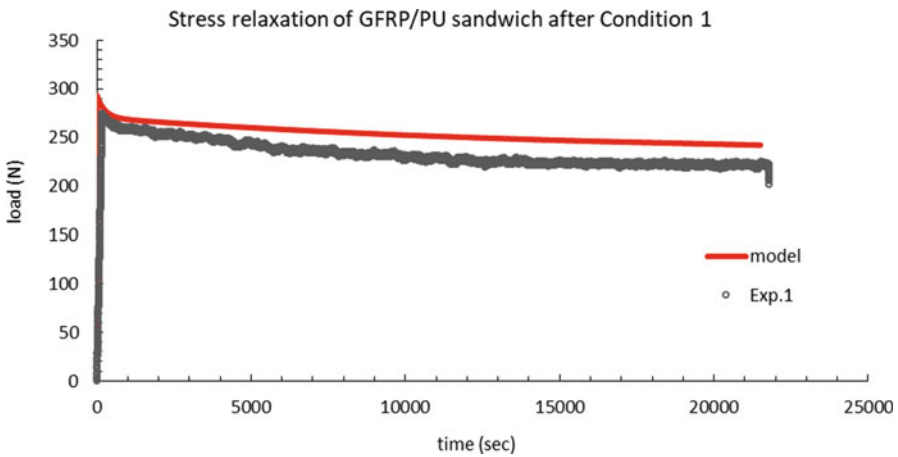


**Fig. 22** Stress relaxation under bending tests (three-point bending) and model of conditioned GFRP/PU sandwich composites
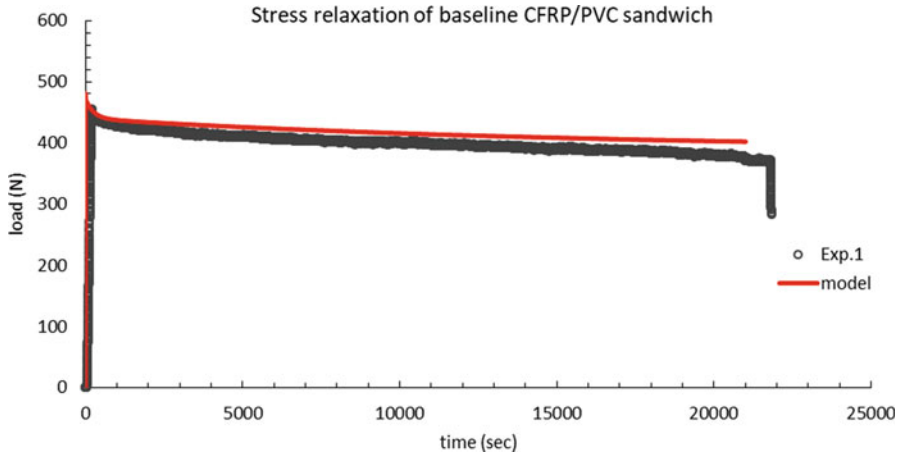
**Fig. 23** Stress relaxation under bending tests (three-point bending) and model of baseline CFRP/PVC sandwich composites



**Fig. 24** Stress relaxation under bending tests (three-point bending) and model of conditioned CFRP/PVC sandwich composites

PVC sandwich composites. Stress relaxation tests and simulations for both baseline and conditioned GFRP/PU and CFRP/PVC sandwich composites are in good agreement with each other. The experimental and FE models of sandwich composites show that we can use the material properties of foam and skin to model the behavior of sandwich composite.

## 5    Conclusions

We have presented a viscoelastic model for predicting the response of sandwich composites subjected to mechanical loading in different environmental conditions, by incorporating different responses of the constituents (skins and foam cores). Experimental tests have been conducted on GFRP and CFRP skins and on PU and PVC foam cores. The purpose of the testing is to calibrate material parameters used in the model. Experimental tests done on sandwich composites are used for validating the model. The model is capable of predicting the behavior of the sandwich composite under mechanical loadings in different environmental conditions, both under quasi-static ramp and creep/relaxation loading conditions.

By investigating the result of the tests and model, we can conclude that the time-dependent response in sandwich composites is mainly due to the viscoelastic response of the foam, while the viscoelastic response of skin is less significant. Also immersion in fluid can alter the mechanical properties of the constituents in sandwich composites, consistent with results in the literature. The mechanical response of baseline sandwich composites can be quite different with respect to that experienced after immersion. Delamination happens in conditioned CFRP/PVC sandwich, while delamination is not seen for the baseline specimen. Furthermore, deformations in the sandwich composites are also governed by the different responses of the constituents (skin and foam core). The GFRP/PU sandwich composites experience foam cracking prior to complete failure, both for the baseline and conditioned samples. As mentioned above CFRP/PVC conditioned sample shows skin-core delamination prior to complete failure. It is shown in this study that the proposed multi-scale model together with a nonlinear viscoelastic constitutive model is capable of describing the overall mechanical response of sandwich composites reasonably well.

## References

1. Sharma N, Gibson RF, Ayorinde EO (2006) Fatigue of foam and honeycomb Core composite Sandwich structures: a tutorial. J Sandw Struct Mater 8:263–319
2. Mouritz AP, Gardiner CP (2002) Compression properties of fire-damage polymer sandwich composites. Compos 33:609–620

3. Siriruk A, Weitsman YJ, Penumadu D (2009) Polymeric foams and sandwich composites: material properties, environmental effects, and shear-lag modeling. Compos Sci Technol 69:814–820

4. Siriruk A, Penumadu D, Weitsman YJ (2009) Effect of sea environment on interfacial delamination behavior of polymeric sandwich structures. Compos Sci Technol 69:821–828

5. Kolat K, Neser |G, Özes C (2007) The effect of sea water exposure on the interfacial fracture of some sandwich systems in marine use. Compos Struct 78:11–17

6. Joshi N, Muliana A (2010) Deformation in viscoelastic sandwich composites subject to moisture diffusion. Compos Struct 92:254–264

7. Du Y, Yan N, Kortschot MT (2013) An experimental study of creep behavior of lightweight natural fiber-reinforced polymer composite/honeycomb core sandwich panels. Compos Struct 106:160–166

8. Shenoi RA, Allen HG, Clark SD (1997) Cyclic creep and creep–fatigue interaction in sandwich beams. J Strain Anal Eng Des 32:1–18

9. Garrido M, Correia JR, Branco FA, Keller T (2014) Creep behaviour of sandwich panels with rigid polyurethane foam core and glass-fibre reinforced polymer faces: experimental tests and analytical modelling. J Compos Mater 48(18):2237–2249

10. Scudamore RJ, Cantwell WJ (2002) The effect of moisture and loading rate on the interfacial fracture properties of Sandwich structures. Polym Compos 23(3):406–417

11. Li X, Weitsman YJ (2004) Sea-water effects on foam-cored composite sandwich lay-ups. Compos Part B 35:451–459

12. Ishai O, Hiel C, Luft M (1995) Long-term hygrothermal effects on damage tolerance of hybrid composite sandwich panels. Compos 26:47–55

13. Degrieck J, Paepegem WV (2001) Fatigue damage modeling of fibre-reinforced composite materials: review. Appl Mech Rev 54(4):279–300

14. Belingardi G, Cavatorta MP, Duella R (2003) Material characterization of a composite–foam sandwich for the front structure of a high speed train. Compos Struct 61:13–25

15. Kim JS, Arronche L, Farrugia A, Muliana A, La Saponara V (2011) Multi-scale modeling of time-dependent response of smart Sandwich constructions. Compos Struct 93:2196–2207

16. Jeon J, Muliana A, La Saponara V (2014) Thermal stress and deformation analyses in Fiber reinforced polymer composites undergoing heat conduction and mechanical loading. Compos Struct 111:31–44

17. Fan Y, Gomez A, Ferraro S, Pinto B, Muliana A, La Saponara V (2017) The effects of temperatures and volumetric expansion on the diffusion of fluids through solid polymers. J Appl Polym Sci 134(31)

18. Fan Y, Gomez A, Ferraro S, Pinto B, Muliana A, La Saponara V (2018) Diffusion of water in glass Fiber reinforced polymer composites at different temperatures. J Compos Mater, in press

19. Fan Y, Gomez A, Muliana A, La Saponara V (2019) Multi-scale analysis of diffusion of fluid in Sandwich composites. J Polym Compos,. in press 40:3520–3532

20. Muliana A, Rajagopal KR (2012) Modeling the response of nonlinear viscoelastic biodegradable polymeric stents. Int J Solids Struct 49:989–1000

21. Fung YC (1981) Biomechanics. In: Mechanical properties of living tissues. Springer, New York

22. Mohr D (2015) "Three dimensional rate-independent plasticity". [Online]. Available: https://www.ethz.ch/

23. "Abaqus Theory anual 4.2.1, Plasticity models: general discussion," [Online]. Available: https://www.sharcnet.ca/Software/Abaqus610/Documentation/docs/v6.10/books/stm/default.htm